

Arithmetic Average Density Fusion - Part III: Heterogeneous Unlabeled and Labeled RFS Filter Fusion

Tiancheng Li, *Senior Member, IEEE*, Ruibo Yan, Kai Da and Hongqi Fan

Abstract—This paper proposes a heterogenous density fusion approach to scalable multisensor multitarget tracking where the inter-connected sensors run different types of random finite set (RFS) filters according to their respective capacity and need. These diverse RFS filters result in heterogenous multitarget densities that are to be fused with each other in a proper means for more robust and accurate detection and localization of the targets. Our approach is based on Gaussian mixture implementations where the local Gaussian components (L-GCs) are revised for PHD consensus, i.e., the corresponding unlabeled probability hypothesis densities (PHDs) of each filter best fit their average regardless of the specific type of the local densities. To this end, a computationally efficient, coordinate descent approach is proposed which only revises the weights of the L-GCs, keeping the other parameters unchanged. In particular, the PHD filter, the unlabeled and labeled multi-Bernoulli (MB/LMB) filters are considered. Simulations have demonstrated the effectiveness of the proposed approach for both homogeneous and heterogenous fusion of the PHD-MB-LMB filters in different configurations.

Index Terms—Random finite set, arithmetic average fusion, heterogenous fusion, PHD consistency, multitarget tracking

I. INTRODUCTION

With the proliferation of internet of things [1], heterogenous sensor networks become promising for multisensor multitarget (MSMT) tracking where the sensors have unequal computing and memory capacities and/or different measurement models and correspondingly run their own suitable algorithms. In fact, it is often required to operate different algorithms even in a homogeneous sensor network, to the prejudice of the network reliability and lifetime [2], [3]. In either case, the local filters are allowed to apply different statistical models (regarding the target birth, detection, survival, and death and the clutter) and approximation algorithms. Thanks to the diversity, the combination of heterogenous filters is naturally more robust and reliable as compared with the unitary one. In this paper, we consider such a heterogenous MSMT tracking problem where (whether homogenous or heterogenous) netted sensors run different types of multitarget filters/trackers derived by

using different families of random finite sets (RFSs) such as unlabeled and labeled RFS filters [4], [5]. Our goal is to find a technically solid means to cooperate these cooperative filters via inter-sensor information fusion for improving their respective, heterogenous estimation.

One solution to the above heterogenous filter cooperation could be given by inter-sensor sharing the raw measurements so that the heterogenous filters just use the aggregated measurements of different sensors. This is particularly useful for dealing with the lack of observability [6], [7] which, however, does not suit the large-scale peer-to-peer networks. More importantly, it is computationally intractable to make the optimal use of the measurements of all sensors due to the explosive possibility for track-to-measurement association [4], [8]–[16]. Differently, we resort to the computationally efficient and scalable density average consensus approach [17] to fuse the probability hypothesis density (PHD) filter [18], [19], the unlabeled multiple Bernoulli (MB) filter [20] and the labeled MB (LMB) filter [21], [22]. It requires only local data communications and simple fusion computation and is proven resilient to complicated/unknown inter-sensor correlation [23], [24]. According to the best of our knowledge, all existing density fusion approaches [17], [25] are homogeneous in the parameter family of the fusing densities, i.e., fusion is carried out among the same type of filters. Note that the defined heterogeneous fusion is different from what given in [26]–[29] where the filters to be fused are still the same type.

Our proposal in this paper is based on the arithmetic-average (AA) density fusion [25], [30], which has recently been tailored to accommodate different RFS densities all demonstrating significant advantages in dealing with misdetection and in high computing efficiency. Effective AA fusion implementations of either unlabeled or labeled RFS filters are all derived from the same (labeled) PHD-AA formulation which ensures consistency in the (labeled) PHD estimation [25] and ultimately more accurate and robust detection and localization of the present targets. This does not only expose the fact that existing linear-fusion-based multi-sensor RFS filters merely seek consensus over the (labeled) PHDs rather than the multi-object probability densities (MPDs) but also paves a way for heterogenous RFS filter cooperation via averaging their respective unlabeled/labeled PHDs as shown in Fig. 1. In view of this, this paper presents the first ever heterogenous unlabeled and labeled RFS filter cooperation approach based on the Gaussian mixture (GM) implementation.

In this paper, the sensors are assumed connected with each

This work was partially supported by National Natural Science Foundation of China (Grant No. 62071389), Natural Science Basic Research Program of Shaanxi Province (Program No. 2023JC-XJ-22), and Key Laboratory Foundation of National Defence Technology (No. JKWATR-210504).

T. Li and R. Yan are with the Key Laboratory of Information Fusion Technology (Ministry of Education), School of Automation, Northwestern Polytechnical University, Xi'an 710129, China, e-mail: t.c.li@nwpu.edu.cn, 2018300490@mail.nwpu.edu.cn

K. Da and H. Fan are with the Key Laboratory of Science and Technology on ATR, National University of Defense Technology, Changsha 410073, China. e-mail: dktm131@163.com, fanhongqi@nudt.edu.cn

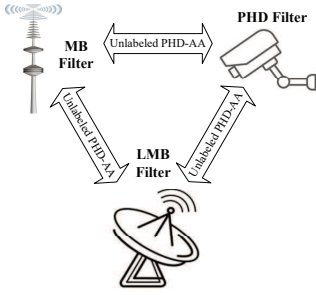


Fig. 1. A heterogeneous RFS filter cooperation scenario based on unlabeled PHD-AA fusion

other either via a centralized fusion center or via a peer-to-peer distributed network. In the latter, the popular average consensus approach [31], [32] or the distributed flooding approach [33] can be used for inter-node communication. The AA density fusion can be easily applied in both cases. Nevertheless, this paper focuses on the centralized fusion for brevity, omitting inter-node communication issues. We further assume that the sensors are synchronous and accurately coordinated, whose fields of view cover the region of interest (ROI). The GM implementations of the local PHD [19], MB [20] and LMB [22] filters are the standard as given in the references in which details are available. These limitations can be relaxed to extend our proposed approach.

The paper is organized as follows. A brief introduction to the Poisson, unlabeled and labeled MBs and their GM implementations are given in sections II and III, respectively. Their heterogeneous fusion performed by merely revising the weights of the local Gaussian components (L-GCs) is given in section IV. Simulation is given in section V before the paper is concluded in section VI.

II. PRELIMINARIES: PHD, MB AND LMB

A. Basic MSMT Scenario

The following scenario assumptions are made in this paper. Target births are independent of target survivals, which might be modelled differently at local sensors based on either Poisson or MB RFSs. Each target evolves and generates measurements independently. At time $k - 1$, the target with state $\mathbf{x}_{k-1} \in \mathcal{X}$ will either die with probability $1 - p_k^s(\mathbf{x}_k)$ or persists at time k with survival probability $p_k^s(\mathbf{x}_k)$ and attains a new state \mathbf{x}_k according to a Markov transition probability density function (PDF) $f_k|\mathbf{x}_{k-1}(\mathbf{x}_k|\mathbf{x}_{k-1})$. Hereafter, $\mathcal{X} \subseteq \mathbb{R}^d$ denotes the d -dimensional state space.

Given a target with state $\mathbf{x}_k \in \mathcal{X}$, sensor $i \in \mathcal{I}$ either detects it with probability $p_{i,k}^d(\mathbf{x}_k)$ and generates a measurement $\mathbf{z}_{i,k} \in Z_{i,k}$ with likelihood $g_{i,k}(\mathbf{z}_{i,k}|\mathbf{x}_k)$ or fails to detect it with probability $1 - p_{i,k}^d(\mathbf{x}_k)$, where $Z_{i,k}$ denotes the set of the measurements received at time k by sensor i . The clutter (namely the measurement of no target) follows a Poisson RFS, independent of target measurements.

B. RFS Modeling

The states of a random number of targets are described by a RFS $X = \{\mathbf{x}_1, \dots, \mathbf{x}_n\} \in \mathbb{X}$, where $n = |X|$ denotes the ran-

dom number of targets and \mathbb{X} denotes all of the finite subsets of \mathcal{X} . For any realization of X with a given cardinality $|X| = n$, namely $X_n = \{\mathbf{x}_1, \dots, \mathbf{x}_n\}$, [4, Eq.2.36], the MPD is defined as $f(X_n) = n! \rho(n) f(\mathbf{x}_1, \dots, \mathbf{x}_n)$ where the localization densities $f(\mathbf{x}_1, \dots, \mathbf{x}_n)$ are symmetric in their arguments and the cardinality distribution is given by $\rho(n) \triangleq \Pr\{|X| = n\} = \int_{|X|=n} f(X) \delta X$. The set integral in \mathbb{X} is defined as [4, Ch. 3.3] $\int_{\mathbb{X}} f(X) \delta X = \sum_{n=0}^{\infty} \frac{1}{n!} \int_{\mathcal{X}^n} f(\{\mathbf{x}_1, \dots, \mathbf{x}_n\}) d\mathbf{x}_1 \dots d\mathbf{x}_n$ where $f(\emptyset) = \rho(0)$.

The PHD $D(\mathbf{x})$, also known as the first moment density [34, pp. 168-169], of the multitarget density $f(X)$ is a density function on single target $\mathbf{x} \in X$, defined as [4, Ch.4.2.8]

$$D(\mathbf{x}) \triangleq \int_{\mathbb{X}} \left(\sum_{\mathbf{y} \in X} \delta_{\mathbf{y}}(\mathbf{x}) \right) f(X) \delta X \quad (1)$$

where $\delta_{\mathbf{y}}(\mathbf{x})$ denotes the Dirac delta function concentrated at \mathbf{y} .

The PHD is the density of the expected cardinality w.r.t. hyper-volume, which has clear physical significance as its integral in any region $\mathcal{S} \subseteq \mathcal{X}$ gives the expected number $\hat{N}^{\mathcal{S}}$ of targets in that region, i.e., $\hat{N}^{\mathcal{S}} = \int_{\mathcal{S}} D(\mathbf{x}) d\mathbf{x}$. Arguably, it tells how well the present targets are detected in the local region. The PHD plays a key role in all RFS filters and undoubtedly, a good PHD estimate implies a good filter estimate. To distinguish the targets, one needs to use the labeled RFS (LRFS) which is a RFS whose elements are assigned with distinct labels [21], [35]. Denote by \mathbb{L} all of the finite subsets of the label space. A realization of a LRFS with cardinality n , multitarget state X_n and label set $L_n = \{l_1, l_2, \dots, l_n\} \in \mathbb{L}$ is denoted by $\tilde{X}_n = \{(\mathbf{x}_1, l_1), (\mathbf{x}_2, l_2), \dots, (\mathbf{x}_n, l_n)\} \in \mathbb{X} \times \mathbb{L}$. The LRFS is completely characterized by its multitarget density $\pi(\tilde{X})$. Consequently, the labeled and unlabeled PHD for a labeled RFS are respectively given as follows [21]

$$\tilde{D}(\mathbf{x}, l) \triangleq \int_{\mathbb{X} \times \mathbb{L}} \pi((\mathbf{x}, l) \cup \tilde{X}) \delta \tilde{X} \quad (2)$$

$$D(\mathbf{x}) \triangleq \sum_{l \in \mathbb{L}} \tilde{D}(\mathbf{x}, l) \quad (3)$$

In this paper, what indicated by the PHD is the unlabeled PHD by default unless otherwise stated.

C. PHD of the Poisson, MB and LMB

We hereafter omit the time notation and the dependence of the filter estimate on the observation process.

1) *Poisson RFS*: The PHD of the Poisson RFS X with mean λ and MPD $f^p(X) = e^{-\lambda} \prod_{\mathbf{x} \in X} \lambda s(\mathbf{x})$ is given by

$$D^p(\mathbf{x}) = \lambda s(\mathbf{x}) \quad (4)$$

where $s(\mathbf{x})$ denotes the single-target probability density (SPD).

2) *MB*: An MB RFS X_n is the union of n independent Bernoulli RFSs [20] which can represent maximum n targets. Denoting the ℓ -th Bernoulli component (BC) by $(r^{(\ell)}, s^{(\ell)}(\mathbf{x}))$, the PHD of MB RFS X_n with the MPD $f^{\text{mb}}(X_n) = \sum_{\cup_{\ell=1}^n X^{(\ell)} = X} \prod_{\ell=1}^n f^{\text{b}}(X^{(\ell)})$ is given by

$$D^{\text{mb}}(\mathbf{x}) = \sum_{\ell=1}^n r^{(\ell)} s^{(\ell)}(\mathbf{x}) \quad (5)$$

where \uplus denotes the disjoint union and the density of a Bernoulli RFS $X^{(\ell)}$ with target existence probability $r^{(\ell)}$ and SPD $s^{(\ell)}(\mathbf{x})$ is given by $f^b(X^{(\ell)}) = 1 - r^{(\ell)}$ if $X^{(\ell)} = \emptyset$, $f^b(X^{(\ell)}) = r^{(\ell)}s^{(\ell)}(\mathbf{x})$ if $X^{(\ell)} = \{\mathbf{x}\}$ and $f^b(X^{(\ell)}) = 0$ otherwise.

3) *LMB*: Similar to the MB filter, the LMB filter [22] associates each labeled BC $l \in L \in \mathbb{L}$ with SPD $s(\mathbf{x}, l)$ and existence probability $r^{(l)}$. The MPD is much complicated as than that for the MB filter, which can be given as $\pi^{\text{lmb}}(\tilde{X}) = \Delta(\tilde{X})\omega(\mathcal{L}(\tilde{X})) \prod_{(\mathbf{x}, l) \in \tilde{X}} s(\mathbf{x}, l)$ where the distinct label indicator $\Delta(\tilde{X}) = \delta_{|\tilde{X}|}(|\mathcal{L}(\tilde{X})|)$, $\delta_I(L) = 1$ if $I = L$ and $\delta_I(L) = 0$ otherwise, the projection function $\mathcal{L}(\mathbb{X} \times \mathbb{L}) \rightarrow \mathbb{L}$ is given by $\mathcal{L}((\mathbf{x}, l)) = l$, $\int_{\mathcal{X}} s(\mathbf{x}, l) d\mathbf{x} = 1$, and $\omega(L)$ denotes the hypothesis weight corresponding to the label set $L \in \mathbb{L}$, which is given by $\omega(L) = \prod_{i \in \mathbb{L}} (1 - r^{(i)}) \prod_{l \in L} \frac{1_{\mathbb{L}}(l)r^{(l)}}{1 - r^{(l)}}$, where $1_{\mathbb{L}}(l) = 1$ if $l \in \mathbb{L}$ and $1_{\mathbb{L}}(l) = 0$ otherwise and $\sum_{L \in \mathbb{L}} \omega(L) = 1$. The labeled and unlabeled PHD of the LMB are respectively given as follows

$$\begin{aligned} \tilde{D}^{\text{lmb}}(\mathbf{x}, l) &= \sum_{L \in \mathbb{L}} 1_L(l) \omega(L) s(\mathbf{x}, l) \\ &= r^{(l)} s(\mathbf{x}, l) \end{aligned} \quad (6)$$

$$\begin{aligned} D^{\text{lmb}}(\mathbf{x}) &= \sum_{l \in \mathbb{L}} \tilde{D}^{\text{lmb}}(\mathbf{x}, l) \\ &= \sum_{l \in \mathbb{L}} r^{(l)} s(\mathbf{x}, l) \end{aligned} \quad (7)$$

D. PHD-AA Consistency

For a set of PHDs $D_i(\mathbf{x})$ produced by RFS filters $i \in \mathcal{I} = \{1, 2, \dots, I\}$, the AA fusion is simply given as follows

$$D_{\text{AA}}(\mathbf{x}) \triangleq \sum_{i \in \mathcal{I}} w_i D_i(\mathbf{x}) \quad (8)$$

where the fusion weights $w_1, \dots, w_I > 0$, $\sum_{i \in \mathcal{I}} w_i = 1$, and the weight space $\mathbb{W} \triangleq \{\mathbf{w} \in \mathbb{R}^I | \mathbf{w}^T \mathbf{1}_I = 1, w_i > 0, \forall i \in \mathcal{I}\}$.

The AA is a Fréchet mean in the sense of the integrated squared difference (ISD) [24], i.e.,

$$D_{\text{AA}}(\mathbf{x}) = \arg \min_{g \in \mathcal{F}_{\mathcal{X}}} \sum_{i \in \mathcal{I}} w_i \int_{\mathcal{X}} (D_i(\mathbf{x}) - g(\mathbf{x}))^2 \delta \mathbf{x} \quad (9)$$

where $\mathcal{F}_{\mathcal{X}} \triangleq \{f : \mathcal{X} \rightarrow \mathbb{R}\}$

Relevantly, it is more known as follows, which we refer to as the best fit of the mixture (BFoM) [36],

$$D_{\text{AA}}(\mathbf{x}) = \arg \min_{g \in \mathcal{F}_{\mathcal{X}}} \sum_{i \in \mathcal{I}} w_i D_{\text{KL}}(D_i || g) \quad (10)$$

where the Kullback-Leibler (KL) divergence, extended to the PHD domain, is defined as $D_{\text{KL}}(f || g) \triangleq \int_{\mathcal{X}} f(\mathbf{x}) \log \frac{f(\mathbf{x})}{g(\mathbf{x})} \delta \mathbf{x}$.

However, in the context of labeled MPD fusion, the labels which suffer more or less from estimate errors conditional on random false/missing data and noises are often different across the sensors. They need to be pairwise-matched between the labeled filters to comply with the track/label-wise fusion rule [25]. Nevertheless, a proper quantitative definition of the divergence/distance between labels is still missing, which is actually the base for label matching. Different labeling

matching choices will in turn lead to very different divergence values and correspondingly different fusion results [37]. To overcome this challenge, the fusion in this work is limited in the unlabeled domain, more precisely unlabeled PHD-AA fusion, which is free of label matching, although the LRFs/LMB filters are involved.

III. GM REPRESENTATIONS OF MB/LMB-PHD

A. GM-PHD

It is theoretically justified and also practically convenient to represent the RFS posterior and at the same time the corresponding PHD by a GM, which facilitates the GM-PHD-AA fusion. Actually, what is estimated and propagated over time in the PHD filter [38] is the PHD, not the MPD. Straightforwardly, the GM approximation of the PHD filter $i \in \mathcal{I}$ at filtering time k can be written as [19]:

$$D_{i,k}(\mathbf{x}) \approx \sum_{j=1}^{J_{i,k}} \omega_{i,k}^{(j)} \mathcal{N}(\mathbf{x}; \boldsymbol{\mu}_{i,k}^{(j)}, \boldsymbol{\Sigma}_{i,k}^{(j)}) \quad (11)$$

where $\mathcal{N}(\mathbf{x}; \boldsymbol{\mu}, \boldsymbol{\Sigma})$ denotes a Gaussian PDF with mean vector $\boldsymbol{\mu}$ and covariance matrix $\boldsymbol{\Sigma}$, $J_{i,k}$ is the number of GCs in total, and $\omega_{i,k}^{(j)}$ is the weight of j th GC at sensor i .

The whole PHD is thereby completely determined by the parameter set $\mathcal{G}_{i,k} \triangleq \{(\omega_{i,k}^{(j)}, \boldsymbol{\mu}_{i,k}^{(j)}, \boldsymbol{\Sigma}_{i,k}^{(j)})\}_{j=1, \dots, J_{i,k}}$. The expected number of targets at sensor $i \in \mathcal{I}$ at time k can be approximated by $\hat{N}_{i,k} = \sum_{j=1}^{J_{i,k}} \omega_{i,k}^{(j)}$.

B. GM Representation of the MB PHD

Consider the GM implementation of the MB posterior represented by a set $L_{i,k}$ of BCs at filtering time k by sensor i . Each BC $(r_{i,k}^{(\ell)}, s_{i,k}^{(\ell)}(\cdot))$, $\ell \in L_{i,k}$ is represented by $J_{i,k}^{(\ell)}$ GCs weighted by $\omega_{i,k}^{(\ell, \iota)} \geq 0$, $\iota = 1, \dots, J_{i,k}^{(\ell)}$, i.e.,

$$s_{i,k}^{(\ell)}(\mathbf{x}) = \sum_{\iota=1}^{J_{i,k}^{(\ell)}} \omega_{i,k}^{(\ell, \iota)} \mathcal{N}(\mathbf{x}; \boldsymbol{\mu}_{i,k}^{(\ell, \iota)}, \boldsymbol{\Sigma}_{i,k}^{(\ell, \iota)}) \quad (12)$$

where

$$\sum_{\iota=1}^{J_{i,k}^{(\ell)}} \omega_{i,k}^{(\ell, \iota)} = 1 \quad (13)$$

Each BC is completely determined by the GM parameter set $\mathcal{G}_{i,k}^{(\ell)} \triangleq \{(\omega_{i,k}^{(\ell, \iota)}, \boldsymbol{\mu}_{i,k}^{(\ell, \iota)}, \boldsymbol{\Sigma}_{i,k}^{(\ell, \iota)})\}_{\iota=1, \dots, J_{i,k}^{(\ell)}}$ by which the PHD (5) is approximated as a set of GMs as follows

$$D_{i,k}(\mathbf{x}) \approx \sum_{\ell \in L_{i,k}} r_{i,k}^{(\ell)} \sum_{\iota=1}^{J_{i,k}^{(\ell)}} \omega_{i,k}^{(\ell, \iota)} \mathcal{N}(\mathbf{x}; \boldsymbol{\mu}_{i,k}^{(\ell, \iota)}, \boldsymbol{\Sigma}_{i,k}^{(\ell, \iota)}) \quad (14)$$

which may be expressed as a unified GM of the parameter set $\mathcal{G}_{i,k} \triangleq \{\mathcal{G}_{i,k}^{(\ell)}\}_{\ell \in L_{i,k}}$ as follows, c.f., (11),

$$D_{i,k}(\mathbf{x}) \approx \sum_{j=1}^{J_{i,k}} \omega_{i,k}^{(j)} \mathcal{N}(\mathbf{x}; \boldsymbol{\mu}_k^{(j)}, \boldsymbol{\Sigma}_k^{(j)}) \quad (15)$$

where $J_{i,k} = \sum_{\ell \in L_{i,k}} J_{i,k}^{(\ell)}$ and the recombined weight of each GC labeled as j is given as

$$\omega_{i,k}^{(j)} = r_{i,k}^{(\ell)} \omega_{i,k}^{(\ell,\ell)} \quad (16)$$

which uses the following unique index mapping at each sensor $i \in \mathcal{I}$ at time k ,

$$j \leftrightarrow (\ell, \ell) \quad (17)$$

where $j = 1, \dots, J_{i,k}, \ell \in L_{i,k}, \ell = 1, \dots, J_{i,k}^{(\ell)}$.

The mean-state of the ℓ -th BC as expressed in (12) is calculated by $\bar{\boldsymbol{\mu}}_{i,k}^{(\ell)} = \sum_{\ell=1}^{J_{i,k}^{(\ell)}} \omega_{i,k}^{(\ell,\ell)} \boldsymbol{\mu}_{i,k}^{(\ell,\ell)}$. By integrating the PHD, the number of targets is estimated at sensor i by

$$\begin{aligned} \hat{N}_{i,k} &= \sum_{\ell \in L_{i,k}} r_{i,k}^{(\ell)} \\ &= \sum_{j=1}^{J_{i,k}} \omega_{i,k}^{(j)} \end{aligned} \quad (18)$$

C. GM Representation of the LMB PHD

The LMB can be viewed as a special MB with assigned label for each BC. That is, with slight abuse of notation and by interpreting each component index ℓ in (12), (14) and (18) as a track label l and set $L_{i,k}$ as the label set of sensor i at time k , the above GM formulation (14) for the MB-PHD can be the same derived for calculating the unlabeled PHD of the LMB. Note that the labels are usually ordered pairs of integers $l = (k, \kappa)$, where k is the time of birth, and κ is a unique index to distinguish new targets born at the same time [21]. The unlabeled PHD $D_{i,k}(\mathbf{x})$ of the local LMB at time k at sensor $i \in \mathcal{I}$, expressed by the parameter set $\mathcal{G}_{i,k} \triangleq \{(\omega_{i,k}^{(j)}, \boldsymbol{\mu}_{i,k}^{(j)}, \boldsymbol{\Sigma}_{i,k}^{(j)})\}_{j=1, \dots, J_{i,k}}$, can be given by, c.f., (15),

$$D_{i,k}(\mathbf{x}) = \sum_{j=1}^{J_{i,k}} \omega_{i,k}^{(j)} \mathcal{N}(\mathbf{x}; \boldsymbol{\mu}_k^{(j)}, \boldsymbol{\Sigma}_k^{(j)}) \quad (19)$$

where multiple L-GCs may have the same label.

IV. GM-PHD FIT VIA OPTIMIZING L-GC WEIGHTS

This paper addresses averaging the PHDs of the PHD, MB, and LMB filters via the GM implementations, where the GM parameter set for time k at sensor $i \in \mathcal{I}$ is denoted by $\mathcal{G}_{i,k}$ and the corresponding local PHD by $D_{i,k}(\mathbf{x})$. The goal of the PHD-AA fusion is to update the local GM parameters so that their corresponding PHDs reach consensus as calculated by (8) in each filtering iteration. As a result, the local filters have similar or the same PHD while their MPDs are variant. A simple 1-D example is given in Fig. 2, where the MB filter has the same PHD as that of the PHD filter while their filter posteriors are heterogeneously parameterized.

Remark 1. *The key challenge to heterogeneous RFS filter fusion origins from the fact that different RFS filters result in different types of MPDs. Unlike the GM-PHD filter, the GCs in the GMs of the MB and of LMB filters intrinsically belong to different (unlabeled or labeled) BCs. Therefore, if a new L-GC is created or an existing L-GC is deleted, one has to identify the BC/label it belongs to.*

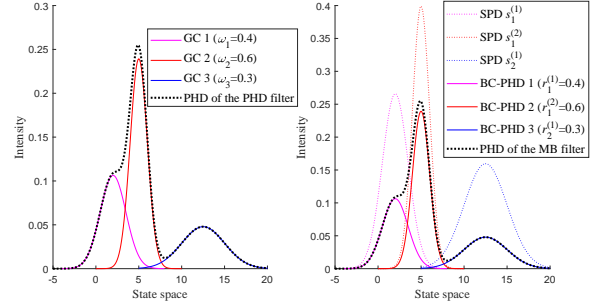


Fig. 2. A MB filter reaches PHD consensus with a PHD filter

The situation is more complicated in the case of MB mixture fusion [36] where the measurement-to-track association hypothesis is further involved. To address this challenge, we hereafter propose an approximate GM-PHD fitting approach which does not create or disregard any L-GCs in the local filters but only optimize their weights $\omega_{i,k}^{(j)}$, $j = 1, \dots, J_{i,k}$ for consensus over their PHDs. Clearly, the resulted PHD is no more than an approximate to the exact PHD-AA. This fit does not only save computation but also enables the parallel-communication-filtering operation similarly as was done in [39], [40] since the mean $\boldsymbol{\mu}_{i,k}^{(j)}$ and covariance $\boldsymbol{\Sigma}_{i,k}^{(j)}$ of each L-GC j , as well as the total number $J_{i,k}$ of L-GCs, are unchanged and therefore can be updated in parallel during the fusion. We omit the detail here. Obviously, better fit can be expected if $\boldsymbol{\mu}_{i,k}^{(j)}$ and $\boldsymbol{\Sigma}_{i,k}^{(j)}$ are also optimized jointly with the weights, regardless of the computational cost.

A. Minimizing ISD of GMs via Reweighting

To evaluate the goodness of fit, the KL divergence can be considered which, however, does not admit analytical solution for the GMs. For the sake of computational efficiency, one may consider the Cauchy-Schwarz divergence [41]¹ and the ISD metric as given in (9), both of which allow analytical calculation for GMs. We consider the latter only, which complies with the BFoM as expressed by (9). Formally speaking, the goal of our approach is to determine the new weight for each L-GC at the local sensor in the following BFoM sense

$$\begin{aligned} \{\omega_{i,k}\}^{\text{BFoM}} &= \arg \min_{\{\omega_{i,k}\} \geq 0} \text{ISD}(D_{i,k} \| D_{\text{AA},k}) \\ &= \arg \min_{\{\omega_{i,k}\} \geq 0} \int \left((1 - w_i) \sum_{j=1}^{J_{i,k}} \omega_{i,k}^{(j)} \mathcal{N}(\mathbf{x}; \boldsymbol{\mu}_{i,k}^{(j)}, \boldsymbol{\Sigma}_{i,k}^{(j)}) \right. \\ &\quad \left. - \sum_{s \in \mathcal{I} \setminus i} w_s \sum_{j=1}^{J_{s,k}} \omega_{s,k}^{(j)} \mathcal{N}(\mathbf{x}; \boldsymbol{\mu}_{s,k}^{(j)}, \boldsymbol{\Sigma}_{s,k}^{(j)}) \right)^2 dx \end{aligned} \quad (20)$$

where $\{\omega_{i,k}^{(j)}\}_{j=1, \dots, J_{i,k}}$ was written as $\{\omega_{i,k}\}$ in short and $A \setminus B$ is the set difference of A and B .

In addition to the above PHD-GM fit, we further communicate and average the multitarget set cardinality estimates

¹It is necessary to note that the Cauchy-Schwarz divergence was originally defined on PDFs and is a normalized distance. Therefore, its application to the PHD is not straightforward but proper extension is needed.

of local sensors for more accurate estimation of the target number, namely cardinality consensus (CC) [42], although the cardinality (distribution) is not directly estimated in the PHD, MB and LMB filters. By using (18), the AA of the estimated number of targets can be calculated as

$$\hat{N}_{AA,k} = \sum_{i \in \mathcal{I}} \hat{N}_{i,k} \quad (22)$$

where $\hat{N}_{i,k} = \sum_{j=1}^{J_k} \omega_{i,k}^{(j)}$ as addressed earlier for the PHD filter in Sec. III-A and for the MB/LMB filters in Sec. III-C.

By taking into account both the non-negative constraint and the above CC constraint of the weights, the GM-weight-fit problem can be formulated as the following constrained multivariate optimization (CMO) problem

$$\min J(\{\omega_{i,k}\}) = \text{ISD}(D_{i,k} \| D_{AA,k}) \quad (23)$$

$$\text{s.t. } \omega_{i,k}^{(j)} \geq 0, j = 1, \dots, J_{i,k} \quad (24)$$

$$\sum_{j=1}^{J_k} \omega_{i,k}^{(j)} = \sum_{j'=1}^{J'_k} \omega_{i',k}^{(j')}, \forall i' \neq i \quad (25)$$

The most challenging issue of the above CMO problem is from the CC constraint (25). To simplify this problem, we address it in a separate step at the end of our algorithm; see section IV-C3. By removing it temporally, the left inequality CMO problem leads to the following Lagrangian function

$$L(\{\omega_{i,k}\}, \{\lambda_j\}) = J(\{\omega_{i,k}\}) - \sum_{j=1}^{J_{i,k}} \lambda_j \omega_{i,k}^{(j)} \quad (26)$$

where $\{\lambda_j\}_{j=1, \dots, J_{i,k}}$ are the Lagrange multipliers.

The Karush-Kuhn-Tucker conditions for this CMO problem are given as follows

$$\frac{\partial J(\{\omega_{i,k}\})}{\partial \omega_{i,k}^{(j)}} - \lambda_j = 0, j = 1, 2, \dots, J_{i,k} \quad (27)$$

$$\lambda_j \omega_{i,k}^{(j)} = 0, j = 1, 2, \dots, J_{i,k} \quad (28)$$

$$\lambda_j \geq 0, j = 1, 2, \dots, J_{i,k} \quad (29)$$

B. A Coordinate Descent CMO Solver and Over-fit

Lemma 1. *Relaxing the non-negative constraint for the weights $\omega_{i,k}^{(j)} \geq 0$, (21) can be solved by, $\forall i \in \mathcal{I}, j = 1, \dots, J_{i,k}$,*

$$\begin{aligned} \omega_{i,k}^{(j),BFoM} = & \\ & \frac{\Delta}{(1 - w_i)} \sum_{s \in \mathcal{I} \setminus i} \sum_{l=1}^{J_{s,k}} w_s \omega_{s,k}^{(l)} \mathcal{N}(\boldsymbol{\mu}_{i,k}^{(j)}; \boldsymbol{\mu}_{s,k}^{(l)}, \boldsymbol{\Sigma}_{i,k}^{(j)} + \boldsymbol{\Sigma}_{s,k}^{(l)}) \\ & - \Delta \sum_{j' \in \mathcal{J}_i^{-j}} \omega_{i,k}^{(j')} \mathcal{N}(\boldsymbol{\mu}_{i,k}^{(j)}; \boldsymbol{\mu}_{i,k}^{(j')}, \boldsymbol{\Sigma}_{i,k}^{(j)} + \boldsymbol{\Sigma}_{i,k}^{(j')}) \end{aligned} \quad (30)$$

where $\Delta = \left| 2 \sum_{i,k}^{(j)} \right|^{1/2} (2\pi)^{d/2}$ and $\mathcal{J}_i^{-j} = \{1, \dots, J_{i,k}\} \setminus j$.

Proof. See Appendix A. The result is from (50). \square

By using (30), we propose a coordinate descent method that sequentially updates the weight of each L-GC $j = 1, \dots, J_{i,k}$

for one or multiple iterations. That is, in iteration $t \in \mathbb{N}^+$, $\omega_{i,k}^{(j')}, j' \in \mathcal{J}_i^{-j}$ in the right hand of (30) is defined as follows for calculating $\omega_{i,k}^{(j,t),BFoM}$,

$$\omega_{i,k}^{(j')} := \begin{cases} \omega_{i,k}^{(j',t)} & j' < j \\ \omega_{i,k}^{(j',t-1)} & j' > j \end{cases} \quad (31)$$

where $\omega_{i,k}^{(j,t)}$ denotes the updated weight of the j th L-GC in iteration t and $\omega_{i,k}^{(j,0)} := \omega_{i,k}^{(j)}$.

The above coordinate descent approach to the CMO problem often suffers from over-fit, i.e., the non-negative constraint $\{\omega_{i,k}\} \geq 0$ is violated or the resulting weight is over-large. This can be addressed as follows, $\forall i \in \mathcal{I}, j = 1, \dots, J_{i,k}$,

$$\tilde{\omega}_{i,k}^{(j,t)} = \max\left(\epsilon, \omega_{i,k}^{(j,t),BFoM}\right) \quad (32)$$

where $\epsilon \geq 0$ is a small constant (e.g., 0.01) specified to avoid generating negative weight.

More importantly, we further take the following strategy to avoid over-fit

$$\omega_{i,k}^{(j,t)} = \alpha_t \tilde{\omega}_{i,k}^{(j,t)} + (1 - \alpha_t) \omega_{i,k}^{(j,t-1)} \quad (33)$$

where $0 < \alpha_t < 1$ is a scaling factor set for iteration t , which can be interpreted as a learning rate.

The learning rate α_t may be set simply fixed. However, there is no guarantee for the sequential fit approach with fixed learning rate α to converge to the optimal solution except that α gradually reduces in a proper means with the increase of t . In the latter, we suggest the following strategy by employing a hyper-parameter β_t

$$\alpha_{t+1} = \beta_t \alpha_t \quad (34)$$

where $0 < \beta_t \leq 1$ can be interpreted as a fading rate and $\beta_t = 1$ means a fixed learning rate.

The above GM-weight-fit iteration based on either fixed or adaptive learning rate may be terminated at a convergence level (i.e., local PHDs approximately reach consensus, e.g., $\text{ISD}(D_{i,k} \| D_{AA,k}) \leq \epsilon$ where ϵ is a small threshold) or up to a maximum number of fit iterations, e.g., $t \leq t_{\max} = 3$.

C. Fusion Feedback

1) *PHD filter:* Each L-GC $j = 1, \dots, J_{i,k}$ of sensor $i \in \mathcal{I}$ that is used for representing the PHD will be simply re-weighted as $\omega_{i,k}^{(j,t)}$ as calculated in (33) after t GM-weight-fit iterations at time k , which can be written as follows

$$\omega_{i,k}^{(j),\text{upd}} = \omega_{i,k}^{(j,t)} \quad (35)$$

2) *MB/LMB filter:* Based on the unique mapping (17), we get the updated, un-normalized weight for l th L-GC of the l th BC/track in sensor i at time k from the fused weight $\omega_{i,k}^{(j,t)}$ as calculated in (33) after t GM-weight-fit iterations as follows

$$\tilde{\omega}_{i,k}^{(\ell,t),\text{upd}} = \omega_{i,k}^{(j,t)} \quad (36)$$

where $j = 1, \dots, J_{i,k}, \ell \in L_{i,k}, l = 1, \dots, J_{i,k}^{(\ell)}$.

According to (13), the weight of the L-GCs in each BC/track should then be normalized, i.e.,

$$\omega_{i,k}^{(\ell,t),\text{upd}} = \frac{\tilde{\omega}_{i,k}^{(\ell,t),\text{upd}}}{\sum_{l=1}^{J_{i,k}^{(\ell)}} \tilde{\omega}_{i,k}^{(l,t),\text{upd}}} \quad (37)$$

3) *CC*: Regardless that the cardinality is not really used for estimating the number of targets in the local MB/LMB filters², it can be used to re-scale the L-GC weights $\omega_{i,k}^{(j)}$, $j = 1, 2, \dots, J_{i,k}$ in the PHD filter and re-scale the track existence probability $r_{i,k}^{(\ell)}$, $\ell \in L_{i,k}$ in the case of MB/LMB filter, respectively, as follows

$$\omega_{i,k}^{(j),\text{upd}} = \frac{\omega_{i,k}^{(j,t)} \hat{N}_{AA,k}}{\hat{N}_{i,k}} \quad (38)$$

$$r_{i,k}^{(\ell),\text{upd}} = \frac{r_{i,k}^{(\ell)} \hat{N}_{AA,k}}{\hat{N}_{i,k}} \quad (39)$$

D. Insufficiency for Track Fusion

The proposed unlabeled PHD-AA suits the most the PHD filter but not the MB/LMB filters due to two reasons

Remark 2. First, the PHD is the first order moment of the MPD for which the PHD-consensus is insufficient for MB/LMB consensus. In other words, two MB/LMB densities can be variant even if their PHDs are the same. This is the limitation of existing RFS-AA fusion approaches based on the consensus of the PHD not of the MPD [25].

Remark 3. Second, the fusion of the MBs/LMBs needs to properly match/associate the BCs that represent latently the same target and then carry out the fusion in each associated group of BCs; see BC-to-BC (B2B) association methods [24], [28] in the homogeneous fusion case. While the B2B-based AA fusion will result in an exactly averaged BC [43], [44], it is, however, inapplicable when fusing the MB/LMB filters with the PHD filters that do not have distinct BCs.

To say the least, the label matching is nontrivial as the labels can be very different with each other among diverse LMB filters. This can be illustrated in Fig. 3 where four GM-LMBs with completely the same GM parameters $\mathcal{G}_i = \mathcal{G}_j$ but different labels $L_i \neq L_j$, $\forall i \neq j$. Different labeling corresponds to different labeled PHDs and different target-state estimates, although their unlabeled PHDs are identical. Overall, our present heterogeneous GM-weight-fit approach overcomes these challenges as it does neither seek track-to-track fusion nor fuse in the labeled domain.

V. SIMULATIONS

We consider a ROI given by $[-1 \text{ km}, 1 \text{ km}] \times [-1 \text{ km}, 1 \text{ km}]$ which is viewed by 4 sensors. The target state is denoted as $\mathbf{x}_k = [x_k \dot{x}_k y_k \dot{y}_k]^T$ with planar position $[x_k y_k]^T$ and velocity $[\dot{x}_k \dot{y}_k]^T$. There are totally 12 targets born at different points as shown in Fig. 4. The target birth is modeled by a MB process with parameters $\{r_B, p_B^{(\ell)}(\cdot)\}_{\ell=1}^4$ at each time-instant, where $r_B = 0.03$, and $p_B^{(\ell)}(\mathbf{x}) = \mathcal{N}(\mathbf{x}; \mu_B^{(\ell)}, \Sigma_B)$ with parameters $\mu_B^{(1)} = [0, 0, 0, 0]^T$, $\mu_B^{(2)} = [400\text{m}, 0, -600\text{m}, 0]^T$, $\mu_B^{(3)} = [-800\text{m}, 0, -200\text{m}, 0]^T$, $\mu_B^{(4)} = [-200\text{m}, 0, 800\text{m}, 0]^T$,

²As usually done in the standard single sensor filter, the number of targets is estimated from the posterior cardinality distribution by taking its mode in the MB filter [20, Sec. III.D] while it depends on the existing probability of each track in comparison with application specific thresholds [22, Sec. IV.E].

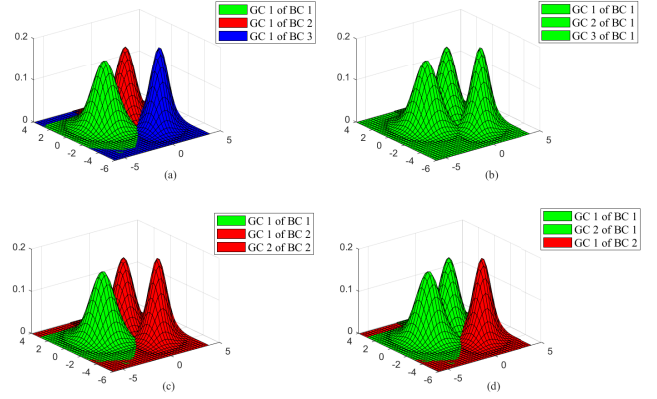


Fig. 3. Four LMBs of the same unlabeled PHD but different labeled PHDs and different potential target-state-estimates.

$\Sigma_B = \text{diag}([10\text{m}, 10\text{m/s}, 10\text{m}, 10\text{m/s}]^T)^2$. We note that this new-born target MB modeling matches the MB/LMB filters but not the PHD filter. In practice, however, it is never known what the ground truth is. The local sensors assume the target birth model based on their own prior knowledge or needs. Both Poisson and MB models are reasonable.

Each target has a constant survival probability 0.95 and follows a constant velocity motion (with the sampling interval $\Delta = 1\text{s}$) using noiseless transition density $f_{k|k-1}(\mathbf{x}_k | \mathbf{x}_{k-1}) = \mathcal{N}(\mathbf{x}_k; F\mathbf{x}_{k-1}, \mathbf{0})$ for generating the ground truth while the filters use $f_{k|k-1}(\mathbf{x}_k | \mathbf{x}_{k-1}) = \mathcal{N}(\mathbf{x}_k; F\mathbf{x}_{k-1}, \mathbf{Q})$, where

$$F = \mathbf{I}_2 \otimes \begin{bmatrix} 1 & \Delta \\ 0 & 1 \end{bmatrix}, \quad \mathbf{Q} = 25 \times \mathbf{I}_2 \otimes \begin{bmatrix} \Delta^2/2 & \Delta/2 \\ \Delta/2 & \Delta \end{bmatrix}$$

where \otimes is the Kronecker product.

The simulation is performed 100 runs with conditionally independent measurement series for 100 seconds each run. In the following, we first consider four sensors with the same time-invariant target detection probability $p_d = 0.9$ and linear measurement model of sensor s as follows

$$\mathbf{z}_{s,k} = \begin{bmatrix} 1 & 0 & 0 & 0 \\ 0 & 0 & 1 & 0 \end{bmatrix} \mathbf{x}_k + \begin{bmatrix} v_{1,k} \\ v_{2,k} \end{bmatrix} \quad (40)$$

with $v_{1,k}$ and $v_{2,k}$ as mutually independent zero-mean Gaussian noise with the same standard deviation of 10m.

We then consider four sensors with the same $p_d = 0.9$ but nonlinear measurement model as follows

$$\mathbf{z}_{s,k} = \begin{bmatrix} \sqrt{(x_k - x^{(s)})^2 + (y_k - y^{(s)})^2} \\ \tan^{-1}\left(\frac{x_k - x^{(s)}}{y_k - y^{(s)}}\right) \end{bmatrix} + \begin{bmatrix} v_{s,k}^{(1)} \\ v_{s,k}^{(2)} \end{bmatrix} \quad (41)$$

where $x^{(s)}$ and $y^{(s)}$ are the coordinates of sensor s which are $[-500\text{m}, -800\text{m}]^T$, $[-500\text{m}, 800\text{m}]^T$, $[600\text{m}, 800\text{m}]^T$ and $[600\text{m}, -800\text{m}]^T$, respectively in our case, $v_{s,k}^{(1)}$ and $v_{s,k}^{(2)}$ are independent zero-mean Gaussian with standard deviation $\sigma_1 = 10\text{m}$ and $\sigma_2 = (\pi/90)\text{rad}$, respectively. The field of view of each sensor is a disk of radius 2km centered at the sensor position $[x^{(s)}, y^{(s)}]^T$ which covers the entire ROI.

In both cases, the clutter measurements of different sensors are independent which uniformly distributed over each sensor's field of view for which the number of clutter points at each scan is Poisson with rate $\kappa_s = 10$.

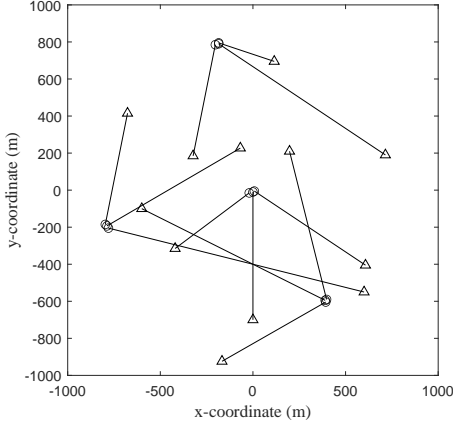


Fig. 4. ROI and target trajectories starting from \circ and ending at \triangle

The filter performance is evaluated by the optimal subpattern assignment (OSPA) error [45], which is given as follows,

$d_{\text{ospa}}^{(c,p)}(\hat{X}, X) = \left((|\hat{X}|)^{-1} (d_{\text{Loc}}(\hat{X}, X) + d_{\text{Card}}(\hat{X}, X)) \right)^{\frac{1}{p}}$ for $|\hat{X}| \geq |X|$, where the localization error (OSPA Loc) and cardinality error (OSPA Card) are defined as $d_{\text{Loc}}(\hat{X}, X) = \min_{\pi \in \Pi_{|\hat{X}|}} \sum_{i=1}^{|\hat{X}|} d^{(c)}(X_i, \hat{x}_{\pi(i)})^p$ and $d_{\text{Card}}(\hat{X}, X) = c^p (|\hat{X}| - |X|)$, respectively. Here, π and Π_n are a permutation and the set of all permutations on $\{1, \dots, n\}$, and $d^{(c)}(X, \mathbf{y}) = \min(d(X, \mathbf{y}), c)$ is a metric between X and \mathbf{y} cut-off at c . If $|\hat{X}| < |X|$, $d_{\text{ospa}}^{(c,p)}(\hat{X}, X) = d_{\text{ospa}}^{(c,p)}(X, \hat{X})$, $d_{\text{Loc}}(\hat{X}, X) = d_{\text{Loc}}(X, \hat{X})$, $d_{\text{Card}}(\hat{X}, X) = d_{\text{Card}}(X, \hat{X})$. In our simulations, we use $c = 100\text{m}$ and $p = 2$.

We consider both homogeneous and heterogeneous fusion cases. In the former, all four sensors run the same PHD, MB or LMB filters, respectively, while in the latter the sensors run different filters. Different levels of fusion have been considered in both cases. They may not cooperate with each other at all (namely noncooperative), only communicate and fuse with each other the estimated number of targets via (38) using $\omega_{i,k}^{(j,t)} = \omega_{i,k}^{(j)}$ or via (39) (namely CC only), or perform the proposed GM-PHD-AA fusion in various numbers of GM-weight-fit iterations, $t = 1, 2, \dots, 6$. We use the learning rate $\alpha_1 = 0.2$ or $\alpha_1 = 0.4$ in (33) and $\beta_t = 0$ (namely fixed learning rate), $\beta_t = 0.6$ (namely adaptive learning rate) in (34), respectively. Furthermore, we use uniform fusing weights, no matter what filters/sensors are involved.

To set up the local filters, the maximum number of L-GCs in the local GM is 200 for the PHD filters, the maximum number of tracks/BCs is 50 and the maximum number of L-GC for each track/BC is 20 in the MB/LMB filters. We note that in practice, these parameters should be designed according to the computational capacity and sensing rate of the local sensors. The other setup of the filters we used, as well as the ground truth, are the same as the standard one as given in the codes released by Vo-Vo at <https://ba-tuong.vo-au.com/codes.html>. Codes for our simulations are available soon in the following URL: sites.google.com/site/tianchengli85/matlab-codes/aa-fusion.

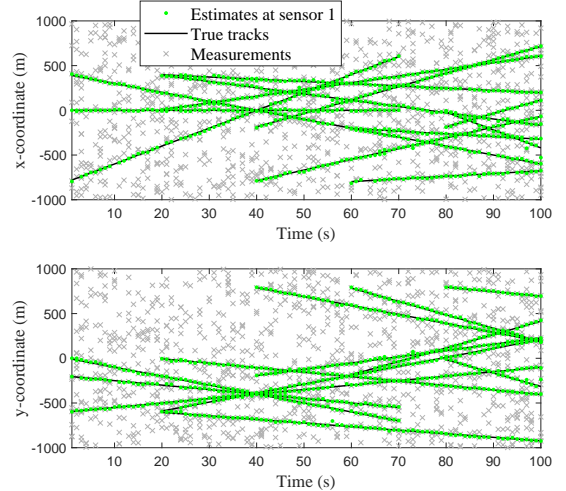


Fig. 5. True tracks, measurements and target position estimates in one run by a local GM-PHD filter

A. Homogeneous PHD/MB/LMB fusion

We first consider the homogeneous PHD filter fusion in order to show the accuracy of the proposed GM fit approach based on the linear measurement model. We also test the standard GM-PHD-AA fusion [46] which averages all of the local GMs. Differently, the size of the local GM is constant in our proposed GM-PHD-fit approach while it increases and so requires appreciate GM reduction such as merging and pruning in the exact GM-PHD-AA fusion. The average OSPA errors, cardinality errors and localization errors over 100 runs for each filtering iteration at four sensors are shown in Fig. 6. The average OSPA errors of the four PHD filters over all 100 runs of 100 filtering steps, by using our proposed GM-weight-fit approach for PHD consensus based on either fixed or adaptive learning rate α_t and by using the standard GM-PHD-AA fusion approach, respectively, have been given in Fig. 7. It shows that the OSPA error has been significantly reduced by the proposed GM-PHD fit approach especially when $\alpha_1 = 0.4, \beta_t = 0.6$ although its reduction is not so significant as the standard GM-PHD-AA fusion does. However, the GM-weight-fit approach using fixed learning rate $\alpha_t = 0.2$ will diverge after $t \geq 4$ but not in the case using adaptive learning rate, although the latter slows down the convergence somehow and results in comparably less OSPA error reduction.

Similarly, we also consider the homogeneous MB filter fusion by using the proposed GM-weight-fit approach for PHD consensus based on either fixed or adaptive learning rate α_t and by using the standard GM-PHD-AA fusion approach [46], respectively, in comparison with the standard MB-AA filter fusion based on the B2B association and inter-sensor GM exchange that enable the parallel Bernoulli-AA fusion, where the B2B association is carried out via the optimal assignment based on the Hungarian algorithm or clustering as addressed in [24]. The average OSPA errors are given in Fig. 8. The results have demonstrated the effectiveness of the proposed, approximate GM-PHD-AA fit approach for fusing these MB filters especially in case of suitable learning rate and fading

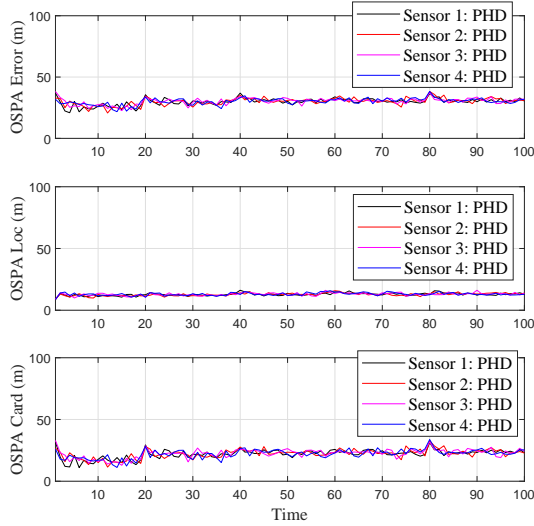


Fig. 6. The OSPA error, cardinality error and localization error of each local PHD filter over time based on only one GM-weight-fit iteration ($\alpha_1 = 0.2$) for PHD consensus

rate, although the fusion gain is much lower than the standard MB-AA fusion. Furthermore, we consider the LMB filters for which the relevant average OSPA results are given in Fig. 9. Compared with the PHD and even the MB filters, the fused LMB filters are improved by the GM-weight-fit approach for PHD consensus much less and is prone to over-fit. It will even deteriorate when $t > 2$ in the case of using fixed $\alpha_t = 0.2$ and even when $t > 1$ in case of over-large adaptive learning rate such as $\alpha_t = 0.4$.

We conjure that better results can be expected in the case of heterogeneous MB and LMB fusion when an appropriate B2B association procedure is employed so that the GM-weight-fit can be performed with regard to each matched/associated BC. To this end, the labels can be removed temporarily so that the LMBs reduce to MBs, which enables BC association/clustering strategies as given for the MB-AA fusion [24]. Overall, the OSPA reduction in the case of MB and LMB filters is lower than that for the PHD filters—as noted in remark 2—and over-fit is easier to occur in the case of using fixed learning rate. Over-fit (non-convergence) has been significantly reduced or even averted by using proper, gradually-decreasing learning rate. These results confirm the analysis given in Section IV-D.

B. Heterogeneous PHD, MB and LMB fusion

This section tests the performance of the proposed GM-AA fit approach in the heterogeneous case. The average results of the proposed GM-AA fit approach for two PHD and two MB filters cooperation, for two PHD and two LMB filters and for two-MB and two-LMB filters cooperation, all filters using adaptive learning rate $\alpha_1 = 0.2, \beta_t = 0.6$, are given in Figs. 10, 11 and 12, respectively. As shown, the heterogeneous fusion reduces the OSPA error of the PHD filters and even the MB filters for which more GM-weight-fit iterations lead to greater reduction of the OSPA error. This confirms the

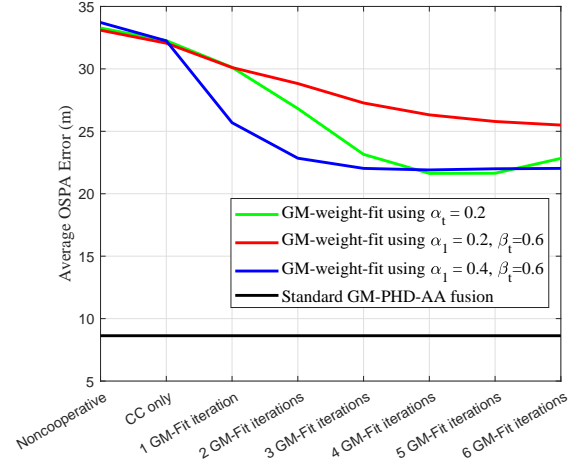


Fig. 7. Average OSPA errors of four PHD filters based on GM-weight-fit for PHD consensus using either fixed or adaptive learning rate in comparison with the standard GM-PHD-AA fusion approach given in [46]

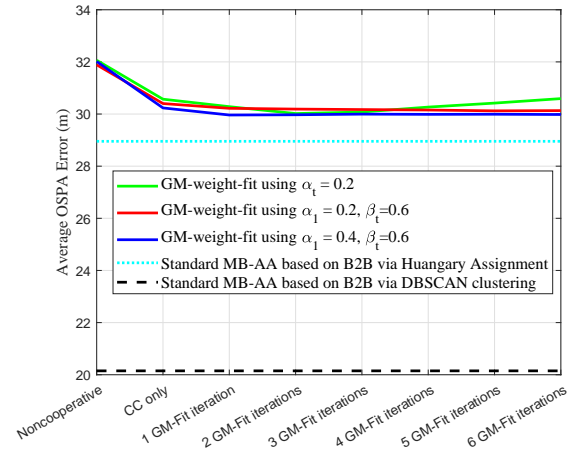


Fig. 8. Average OSPA errors of four MB filters based on GM-weight-fit for PHD consensus using either fixed or adaptive learning rate in comparison with the standard MB-AA filters [24] based on two different B2B association strategies respectively

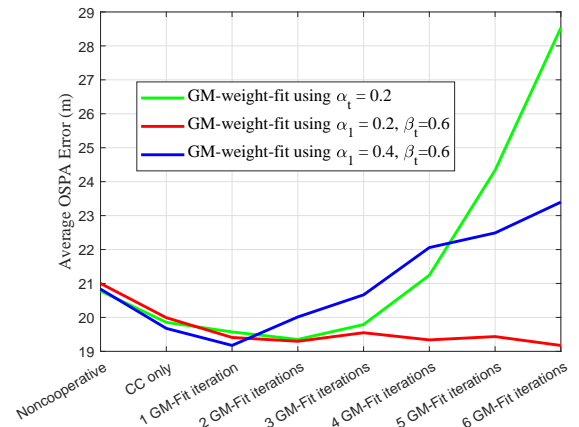


Fig. 9. Average OSPA errors of four LMB filter based on GM-weight-fit for PHD consensus using either fixed or adaptive learning rate

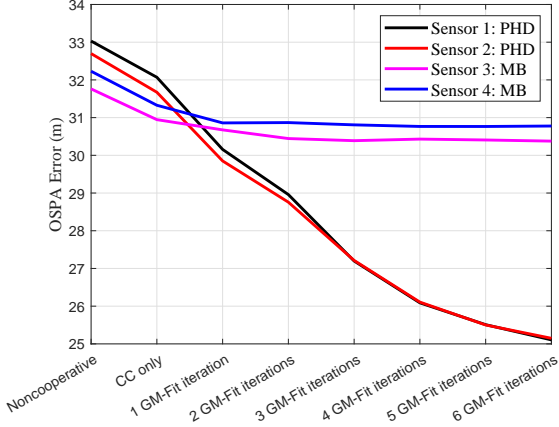


Fig. 10. The OSPA errors of two PHD and two MB filters against different levels of GM-weight-fit using adaptive learning rate $\alpha_1 = 0.2$, $\beta_t = 0.6$

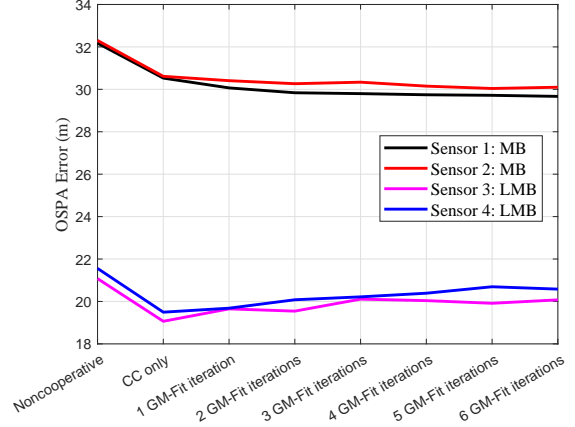


Fig. 12. The OSPA errors of two MB and two LMB filters against different levels of GM-weight-fit using adaptive learning rate $\alpha_1 = 0.2$, $\beta_t = 0.6$

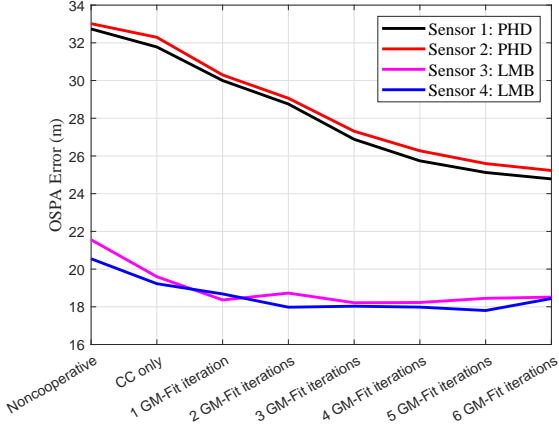


Fig. 11. The OSPA errors of two PHD and two LMB filters against different levels of GM-weight-fit using adaptive learning rate $\alpha_1 = 0.2$, $\beta_t = 0.6$

effectiveness of the proposed approach for heterogeneous RFS filter fusion. Similar to the case of homogeneous fusion in section V-A, the proposed GM-AA fit approach improves the PHD filter more than the MB/LMB filter when they are fused with each other. However, surprisingly, the heterogeneous fusion with the MB filter does not benefit the LMB filter more than the CC-only strategy, which means the proposed sequential GM-weight-fit does not improve the LMB filter except the CC part. This is mainly due to the lack of B2B association as addressed in Section IV-D. To address it, the fusion needs to be carried out in a track-wise fashion for which appropriate B2B association across sensors is required. We leave this to the future work.

We further consider a more complicated configuration of two PHD filters, one MB filter and one LMB filter. The average OSPA error of each filter based on the proposed GM-weight-fit approach for PHD consensus is given in Fig. 13, which confirms that the heterogeneous unlabeled PHD-AA fusion based on GM-weight-fit improve all filters, especially the PHD filters. However, it remains open how to best set the learning rate, the fading rate as well as the number of GM-weight-fit iterations for each filter in different cooperation

configures. According to our experience, a rule of thumb choice is $\alpha_1 = 0.2$, $\beta_t = 0.6$.

Moreover, the average computing times costed by one iteration of the PHD, MB, LMB filtering operation separately and by their fusion operation with different numbers of GM-weight-fit iterations are also given in Fig. 13. As shown, the proposed GM-weight-fit approach is computing more costly as compared with the filtering operations in general due to the intensive computation for calculating the correlation among all GCs as in (30). However, the computation time required increase slowly with the increase of the number of GM-weight-fit iterations. This is because the correlation between GCs only needs to be calculated once (and be recorded for multiple uses in different iterations) because the means and variances of the GCs are unchanged.

Finally, we test the heterogeneous fusion of two PHD filters, one MB filter and one LMB filter based on the nonlinear measurement model (41) for which the local filters employ the unscented approximation for dealing with the nonlinearity. The average OSPA errors and average computing times for one filtering iteration of each filter and for their heterogeneous fusion are given in Fig. 14, respectively. The results comply with those in the linear measurement case. Differently, the two PHD filters that are localized at different positions which are related to their respective range-bearing measurements perform quite differently with each other, although both of them are improved by the heterogeneous fusion more significantly as compared with the MB and LMB filters.

VI. CONCLUSION AND FUTURE WORK

We propose a heterogeneous unlabeled and labeled RFS filter fusion approach which averages the unlabeled PHDs of the diverse RFS filters based on the GM implementation. A computationally efficient, approximate approach to GM weight fit is proposed which sequentially revises only the weights of the Gaussian components of the local GM in multiple iterations for PHD consensus. Both fixed and adaptive parameters have been suggested for controlling the convergence of the proposed fitting approach. Simulations have demonstrated the

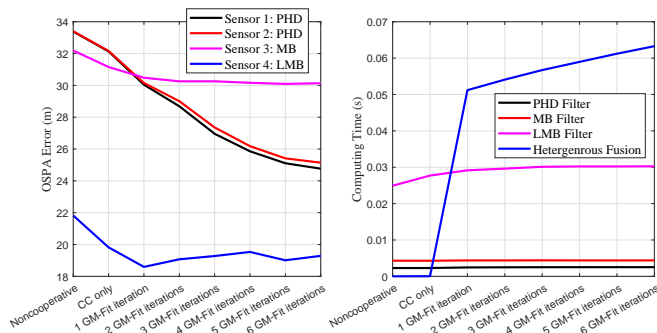


Fig. 13. Linear measurement case: the OSPA errors and average computing time for each filtering step of two PHD, one MB and one LMB filters, and their heterogeneous fusion time against different levels of GM-weight-fit using adaptive learning rate $\alpha_1 = 0.2, \beta_t = 0.6$

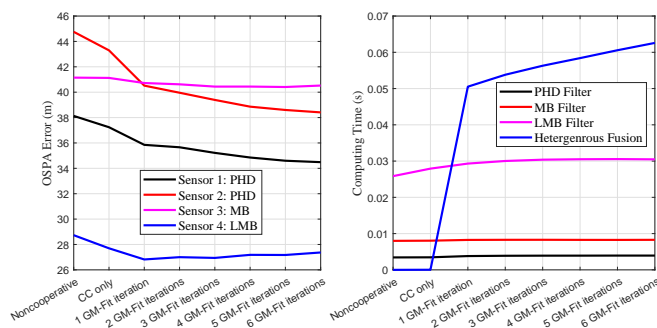


Fig. 14. Nonlinear measurement case: the OSPA errors and average computing time for each filtering step of two PHD, one MB and one LMB filters, and their heterogeneous fusion time against different levels of GM-weight-fit using adaptive learning rate $\alpha_1 = 0.2, \beta_t = 0.6$

effectiveness of the proposed approach using adaptive fitting parameters for both homogeneous and heterogeneous PHD-MB-LMB filter fusion. Our approach improves the PHD filter significantly by cooperating with the MB/LMB filters or the other PHD filters. In comparison, it improves the MB and LMB filters less. The reasons are twofold. First, the PHD is only the first order moment of the MB/LMB density for which the PHD-consensus is insufficient for MB/LMB consensus. Second, the proposed heterogeneous fusion is carried out in the unlabeled domain which applies no track/label matching for track-wise fusion. This leaves great space for further improvement.

Improvement can be expected if more parameters of the L-GCs such as the means and covariances can be jointly optimized with the weights for better GM-fit and if the BCs can be properly associated (or the labels can be properly matched) in the case of MB/LMB filter for B2B-based PHD fusion. To this end, advanced approximation/optimization methods such as variational Bayes and expectation maximization can be considered. However, label/track matching/association remains an open-ended, challenging issue even for homogeneous MB/LMB filter fusion and needs further investigation. Valuable future works also include addressing the partially overlapping field of view of the sensors, unknown target birth/dynamics/death models, unknown sensor profiles (such as the target detection probability and clutter rate) and so on

based on the framework of the heterogeneous fusion.

APPENDIX

A. Partial differential of the ISD of GMs

The ISD between two GMs $p(\mathbf{x}) = \sum_{n \in \mathbf{I}_1} \alpha_n \mathcal{N}(\mathbf{x}; \boldsymbol{\mu}_n, \mathbf{P}_n), q(\mathbf{x}) = \sum_{m \in \mathbf{I}_2} \beta_m \mathcal{N}(\mathbf{x}; \mathbf{m}_m, \mathbf{S}_m)$ is given as follows [47]

$$\text{ISD}(p||q) \triangleq \int (p(\mathbf{x}) - q(\mathbf{x}))^2 d\mathbf{x} \quad (42)$$

$$= \text{ISD}_\alpha + \text{ISD}_\beta - 2\text{ISD}_{\alpha\beta} \quad (43)$$

where

$$\text{ISD}_\alpha = \sum_{n, n' \in \mathbf{I}_1} \alpha_n \alpha_{n'} \mathcal{N}(\boldsymbol{\mu}_n; \boldsymbol{\mu}_{n'}, \mathbf{P}_n + \mathbf{P}_{n'}) \quad (44)$$

$$\text{ISD}_\beta = \sum_{m, m' \in \mathbf{I}_2} \beta_m \beta_{m'} \mathcal{N}(\mathbf{m}_m; \mathbf{m}_{m'}, \mathbf{S}_m + \mathbf{S}_{m'}) \quad (45)$$

$$\text{ISD}_{\alpha\beta} = \sum_{n \in \mathbf{I}_1, m \in \mathbf{I}_2} \alpha_n \beta_m \mathcal{N}(\boldsymbol{\mu}_n; \mathbf{m}_m, \mathbf{P}_n + \mathbf{S}_m) \quad (46)$$

Here, it is straightforward to derive that

$$\begin{aligned} \frac{\partial \text{ISD}(p||q)}{\partial \alpha_n} &= 2 \sum_{n' \neq n, n' \in \mathbf{I}_1} \alpha_{n'} \mathcal{N}(\boldsymbol{\mu}_n; \boldsymbol{\mu}_{n'}, \mathbf{P}_n + \mathbf{P}_{n'}) \\ &\quad + 2\alpha_n \mathcal{N}(\boldsymbol{\mu}_n; \boldsymbol{\mu}_n, 2\mathbf{P}_n) \\ &\quad - 2 \sum_{m \in \mathbf{I}_2} \beta_m \mathcal{N}(\boldsymbol{\mu}_n; \mathbf{m}_m, \mathbf{P}_n + \mathbf{S}_m) \end{aligned} \quad (47)$$

$$\begin{aligned} \frac{\partial^2 \text{ISD}(p||q)}{\partial \alpha_n^2} &= 2\mathcal{N}(\boldsymbol{\mu}_n; \boldsymbol{\mu}_n, 2\mathbf{P}_n) \\ &= \frac{2}{|\mathbf{2P}_n|^{1/2} (2\pi)^{d/2}} \\ &> 0 \end{aligned} \quad (48)$$

Setting (47) zero will lead to

$$\begin{aligned} \alpha_n &= |\mathbf{2P}_n|^{1/2} (2\pi)^{d/2} \sum_{m \in \mathbf{I}_2} \beta_m \mathcal{N}(\boldsymbol{\mu}_n; \mathbf{m}_m, \mathbf{P}_n + \mathbf{S}_m) \\ &\quad - |\mathbf{2P}_n|^{1/2} (2\pi)^{d/2} \sum_{n' \neq n} \alpha_{n'} \mathcal{N}(\boldsymbol{\mu}_n; \boldsymbol{\mu}_{n'}, \mathbf{P}_n + \mathbf{P}_{n'}) \end{aligned} \quad (50)$$

which yields the minimum ISD given all the other L-GC weights $\{\alpha_{n'}\}_{n' \neq n, n' \in \mathbf{I}_1}, \{\beta\}_{m \in \mathbf{I}_2}$.

ACKNOWLEDGEMENT

The authors would like to thank the anonymous reviewers for their constructive and detailed comments, which motivated the idea of designing the adaptive learning rate in the proposed GM-weight-fit approach for PHD consensus.

REFERENCES

- [1] T. Qiu, N. Chen, K. Li, M. Atiquzzaman, and W. Zhao, "How can heterogeneous internet of things build our future: A survey," *IEEE Communications Surveys & Tutorials*, vol. 20, no. 3, pp. 2011–2027, 2018.
- [2] M. Yarvis, N. Kushalnagar, H. Singh, A. Rangarajan, Y. Liu, and S. Singh, "Exploiting heterogeneity in sensor networks," in *Proceedings IEEE 24th Annual Joint Conference of the IEEE Computer and Communications Societies.*, vol. 2, 2005, pp. 878–890 vol. 2.
- [3] M. Liggins, D. Hall, and J. Llinas, *Handbook of Multisensor Data Fusion: Theory and Practice, Second Edition*, ser. Electrical Engineering & Applied Signal Process. Series. Boca Raton, FL, USA: CRC Press, 2017.
- [4] R. Mahler, *Advances in Statistical Multisource-Multitarget Information Fusion*. Artech House, 2014.
- [5] B.-N. Vo, M. Mallick, Y. Bar-shalom, S. Coraluppi, R. Osborne, R. Mahler, and B.-T. Vo, "Multitarget tracking," in *Wiley Encyclopedia of Electrical and Electronics Engineering*. John Wiley & Sons, 2015.
- [6] D. Hamidi, E. Kevelevitch, P. Arora, R. Gentile, and V. Pellissier, "Angle-only, range-only and multistatic tracking based on GM-PHD filter," in *Proceedings of FUSION 2021*, 2021, pp. 1–8.
- [7] Y. Xie and T. L. Song, "Bearings-only multi-target tracking using an improved labeled multi-Bernoulli filter," *Signal Processing*, vol. 151, pp. 32–44, 2018.
- [8] E. Delande, E. Duflos, P. Vanheeghe, and D. Heurquier, "Multi-sensor PHD: Construction and implementation by space partitioning," in *Proc. Int. Conf. Control Autom. Inf. Sci.*, 2011, pp. 3632–3635.
- [9] S. Nannuru, S. Blouin, M. Coates, and M. Rabbat, "Multisensor CPHD filter," *IEEE Trans. Aerosp. Electron. Syst.*, vol. 52, no. 4, pp. 1834–1854, 2016.
- [10] B. Wei, B. Nener, W. Liu, and L. Ma, "Centralized multi-sensor multi-target tracking with labeled random finite sets," in *Proc. IEEE Int. Conf. Control, Auto. Inf. Sci.*, 2016, pp. 82–87.
- [11] A.-A. Saucan, M. J. Coates, and M. Rabbat, "A multisensor multi-Bernoulli filter," *IEEE Trans. Signal Process.*, vol. 65, no. 20, pp. 5495–5509, 2017.
- [12] B.-N. Vo, B.-T. Vo, and M. Beard, "Multi-sensor multi-object tracking with the generalized labeled multi-Bernoulli filter," *IEEE Trans. Signal Process.*, vol. 67, no. 23, pp. 5952–5967, 2019.
- [13] W. Si, H. Zhu, and Z. Qu, "Multi-sensor Poisson multi-Bernoulli filter based on partitioned measurements," *IET Radar, Sonar Navig.*, vol. 14, no. 6, pp. 860–869, 2020.
- [14] S. Robertson, C. van Daalen, and J. du Preez, "Efficient approximations of the multi-sensor labelled multi-bernoulli filter," *Signal Processing*, vol. 199, p. 108633, 2022.
- [15] A. Trezza, D. J. Bucci, and P. K. Varshney, "Multi-sensor joint adaptive birth sampler for labeled random finite set tracking," *IEEE Transactions on Signal Processing*, vol. 70, pp. 1010–1025, 2022.
- [16] D. Moratuwage, B.-N. Vo, B.-T. Vo, and C. Shim, "Multi-scan multi-sensor multi-object state estimation," *IEEE Transactions on Signal Processing*, vol. 70, pp. 5429–5442, 2022.
- [17] T. Li, K. Da, H. Fan, and B. Yu, "Multisensor random finite set information fusion: Advances, challenges, and opportunities," in *Secure and Digitalized Future Mobility: Shaping the Ground and Air Vehicles Cooperation*, Y. Cao, O. Kaiwartya, and T. Li, Eds. CRC Press, Nov. 2022.
- [18] B.-N. Vo, S. Singh, and A. Doucet, "Sequential Monte Carlo methods for multitarget filtering with random finite sets," *IEEE Trans. Aerosp. Electron. Syst.*, vol. 41, no. 4, pp. 1224–1245, Oct. 2005.
- [19] B. N. Vo and W. K. Ma, "The Gaussian mixture probability hypothesis density filter," *IEEE Trans. Signal Process.*, vol. 54, no. 11, pp. 4091–4104, Nov 2006.
- [20] B.-N. Vo, B.-T. Vo, and A. Cantoni, "The cardinality balanced multi-target multi-Bernoulli filter and its implementations," *IEEE Trans. Signal Process.*, vol. 57, no. 2, pp. 409–423, Feb. 2009.
- [21] B.-T. Vo and B.-N. Vo, "Labeled random finite sets and multi-object conjugate priors," *IEEE Trans. Signal Process.*, vol. 61, no. 13, pp. 3460–3475, Jul. 2013.
- [22] S. Reuter, B.-T. Vo, B.-N. Vo, and K. Dietmayer, "The labeled Multi-Bernoulli filter," *IEEE Trans. Signal Processing*, vol. 62, no. 12, pp. 3246–3260, 2014.
- [23] T. Bailey, S. Julier, and G. Agamennoni, "On conservative fusion of information with unknown non-Gaussian dependence," in *Proc. FUSION 2012*, Singapore, Jul. 2012, pp. 1876–1883.
- [24] T. Li, X. Wang, Y. Liang, and Q. Pan, "On arithmetic average fusion and its application for distributed multi-Bernoulli multitarget tracking," *IEEE Trans. Signal Process.*, vol. 68, pp. 2883–2896, 2020.
- [25] T. Li, "Arithmetic average density fusion - part ii: Unified derivation for (labeled) RFS fusion," 2022, preprint: arXiv:2209.10433.
- [26] A. Petitti, D. Di Paola, A. Rizzo, and G. Cicarelli, "Consensus-based distributed estimation for target tracking in heterogeneous sensor networks," in *2011 50th IEEE Conference on Decision and Control and European Control Conference*, 2011, pp. 6648–6653.
- [27] O. Dagan and N. R. Ahmed, "Heterogeneous decentralized fusion using conditionally factorized channel filters," in *2020 IEEE International Conference on Multisensor Fusion and Integration for Intelligent Systems (MFI)*, 2020, pp. 46–53.
- [28] W. Yi and L. Chai, "Heterogeneous multi-sensor fusion with random finite set multi-object densities," *IEEE Transactions on Signal Processing*, vol. 69, pp. 3399–3414, 2021.
- [29] S. Arulampalam, B. Ristic, and T. Kirubarajan, "Analysis of propagation delay effects on bearings-only fusion of heterogeneous sensors," *IEEE Transactions on Signal Processing*, vol. 69, pp. 6488–6503, 2021.
- [30] T. Li, Y. Song, E. Song, and H. Fan, "Arithmetic average density fusion - part i: Some statistic and information-theoretic results," *Information Fusion*, 2021, arXiv:2110.01440.
- [31] R. Olfati-Saber, J. A. Fax, and R. M. Murray, "Consensus and cooperation in networked multi-agent systems," *Proc. IEEE*, vol. 95, no. 1, pp. 215–233, Jan. 2007.
- [32] A. H. Sayed, "Adaptation, learning, and optimization over networks," *Found. Trends in Machine Learn.*, vol. 7, no. 4-5, pp. 311–801, 2014.
- [33] T. Li, J. Corchado, and J. Prieto, "Convergence of distributed flooding and its application for distributed Bayesian filtering," *IEEE Trans. Signal Inf. Process. Netw.*, vol. 3, no. 3, pp. 580–591, Sep. 2017.
- [34] I. R. Goodman, R. P. S. Mahler, and H. T. Nguyen, *Mathematics of Data Fusion*. Springer Dordrecht, 1997.
- [35] B.-T. Vo, B.-N. Vo, and D. Phung, "Labeled random finite sets and the Bayes multi-target tracking filter," *IEEE Trans. Signal Process.*, vol. 62, no. 24, pp. 6554–6567, Dec. 2014.
- [36] T. Li, Y. Xin, Z. Liu, and K. Da, "Best fit of mixture for computationally efficient poisson multi-Bernoulli mixture filtering," *Signal Processing*, vol. 202, p. 108739, 2023.
- [37] T. Li, H. Liang, B. Xiao, Q. Pan, and Y. He, "Finite mixture modeling in time series: A survey of bayesian filters and fusion approaches," *Information Fusion*, 2023.
- [38] R. P. S. Mahler, "Multitarget Bayes filtering via first-order multitarget moments," *IEEE Trans. Aerosp. Electron. Syst.*, vol. 39, no. 4, pp. 1152–1178, Oct. 2003.
- [39] T. Li and F. Hlawatsch, "A distributed particle-PHD filter using arithmetic-average fusion of Gaussian mixture parameters," *Information Fusion*, vol. 73, pp. 111–124, 2021.
- [40] T. Li, M. Mallick, and Q. Pan, "A parallel filtering-communication based cardinality consensus approach for real-time distributed PHD filtering," *IEEE Sensors J.*, vol. 20, no. 22, pp. 13 824–13 832, 2020.
- [41] K. Kampa, E. Hasanbelliu, and J. C. Principe, "Closed-form Cauchy-Schwarz PDF divergence for mixture of Gaussians," in *The 2011 International Joint Conference on Neural Networks*, 2011, pp. 2578–2585.
- [42] T. Li, F. Hlawatsch, and P. M. Djuric, "Cardinality-consensus-based PHD filtering for distributed multitarget tracking," *IEEE Signal Process. Lett.*, vol. 26, no. 1, pp. 49–53, Jan. 2019.
- [43] K. Da, T. Li, Y. Zhu, H. Fan, and Q. Fu, "Kullback-Leibler averaging for multitarget density fusion," in *Proc. DCAI 2019*, Avila, Spain, Jun. 2019, pp. 253–261.
- [44] T. Li, Z. Liu, and Q. Pan, "Distributed Bernoulli filtering for target detection and tracking based on arithmetic average fusion," *IEEE Signal Processing Letters*, vol. 26, no. 12, pp. 1812–1816, Dec. 2019.
- [45] D. Schuhmacher, B.-T. Vo, and B.-N. Vo, "A consistent metric for performance evaluation of multi-object filters," *IEEE Trans. Signal Process.*, vol. 56, no. 8, pp. 3447–3457, Aug. 2008.
- [46] T. Li, J. Corchado, and S. Sun, "Partial consensus and conservative fusion of Gaussian mixtures for distributed PHD fusion," *IEEE Trans. Aerosp. Electron. Syst.*, vol. 55, no. 5, pp. 2150–2163, Oct. 2019.
- [47] J. L. Williams and P. S. Maybeck, "Cost-function-based hypothesis control techniques for multiple hypothesis tracking," *Math Comput Model.*, vol. 43, no. 9-10, pp. 976–989, 2006.